The Laplacian of Electron Density versus NICSzz Scan: Measuring Magnetic Aromaticity among Molecules with Different Atom Types

ARTICLE *in* THE JOURNAL OF PHYSICAL CHEMISTRY A · JULY 2011

Impact Factor: 2.69 · DOI: 10.1021/jp203681x · Source: PubMed

4 AUTHORS, INCLUDING:

Cina Foroutan-Nejad
Masaryk University
29 PUBLICATIONS **243** CITATIONS
SEE PROFILE

Shant Shahbazian
Shahid Beheshti University
52 PUBLICATIONS **563** CITATIONS
SEE PROFILE

Parviz Rashidi
University of Tehran
52 PUBLICATIONS **377** CITATIONS
SEE PROFILE

THE JOURNAL OF PHYSICAL CHEMISTRY A

ARTICLE

pubs.acs.org/JPCA

The Laplacian of Electron Density versus $NICS_{zz}$ Scan: Measuring Magnetic Aromaticity among Molecules with Different Atom Types

Cina Foroutan-Nejad,[†] Zahra Badri,[†] Shant Shahbazian,[‡] and Parviz Rashidi-Ranjbar*[,†]

[†]School of Chemistry, College of Science, University of Tehran, Tehran, Iran

[‡]Department of Chemistry, Faculty of Sciences, Shahid Beheshti University, G.C., Evin, Tehran, Iran

Supporting Information

ABSTRACT: The electron density versus $NICS_{zz}$ (the out-of-plane component of nucleus-independent chemical shifts (NICS)) scan for assessing magnetic aromaticity among similar molecules with different ring sizes is improved by scanning the Laplacian of electron density versus $NICS_{zz}$ to include molecules containing different types of atoms. It is demonstrated that the new approach not only reproduces the results of the previous method but also surpasses that in the case of species with different atom types. The relative positions of curves in the plots of the Laplacian of electron density versus $NICS_{zz}$ correlate well with the ring current intensities of these molecules both near and far from the ring planes of the considered molecules. Accordingly, relative magnetic aromaticity of a number of planar hydrocarbons and a group of double aromatic metallic/semimetallic species are studied and discussed.

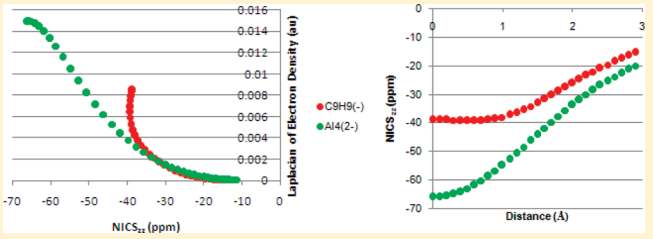

INTRODUCTION

After about 150 years, aromaticity still remains an interesting and useful concept for chemical community.[1] In modern chemistry, not only is this concept not considered old fashioned, but it also has been extended to new horizons, e.g., all-metal aromatic species,[2] which were not imaginable in the 19th century. Additionally, continuous progress in quantum chemical methods provides new approaches probing the extent of aromaticity in different aromatic molecules.[3]

Among different probes, the electronic as well as magnetic criteria of aromaticity have been vastly employed in recent years.[4] However, a heedful survey of the relevant literature reveals the fact that there is no general agreement between the outcomes of different magnetic probes on the extent of relative magnetic aromaticity, i.e., the relative strength of diatropic ring currents of aromatic species.[5] However, there are scattered reports that try to clarify the origin of the divergence of different magnetic indices of aromaticity.[6]

Since 1996, nucleus-independent chemical shifts (NICS)[7] has been the most popular magnetic probe of aromaticity; its vast application is mostly due to its ease of computation and interpretation. This probe has been several times revised, and different modified variants of the NICS have been introduced thereafter (a brief survey on the evolution of various NICS variants may be found in ref 5f).[5f,6a−6c,8] Recently, we have demonstrated that for a number of organic aromatic molecules with different ring sizes, considering the diagrams of one-electron density versus the NICS considerably improves the description of the relative magnetic aromaticity.[5f] Moreover, our recent studies demonstrate that any type of single-point NICS and even NICS scan methodology cannot verify the correct order of magnetic aromaticity among a number of all-metal aromatic clusters as well as planar hydrocarbons.[6e] It was shown that the NICS deficiency originates from the differences in the electron density distribution in molecules with different ring sizes and various atom types.[6e]

Beside the electron density, the Laplacian of the electron density, $\nabla^2\rho$, may play a very similar role for determining the order of aromaticity since $\nabla^2\rho$ serves as a magnifier allowing one to trace the fine pattern of the electron density distribution and provides a variety of information regarding this distribution that is not easily available from studying ρ itself. Therefore, the application of $\nabla^2\rho$ instead of ρ may hopefully be more informative in order to determine the relative aromaticity. However, this hypothesis should be practically examined since there is no simple mathematical relationship between the one-electron density or its derivatives and the non-nuclear (or nuclear) magnetic shieldings (for a discussion on a theoretical link, not yet practical, based on the Hohenberg−Kohn theorem, see ref 5f). Indeed, the situation in this study is more or less similar in spirit to the formulation of approximate exchange-correlation functionals in the computational density functional theory (DFT); one knows that there is a link in principle, but there is no easy way to determine the link, so one must test various reasonable approximations.

Special Issue: Richard F. W. Bader Festschrift

Received: April 20, 2011
Revised: June 2, 2011
Published: July 01, 2011

Accordingly, a number of molecules whose relative magnetic aromaticity was determined before[6e] are selected to be studied based on the scan of $\nabla^2\rho$ versus the NICS. Thus, the aim of this paper is introducing the application of the Laplacian of electron density as an auxiliary probe to reveal the fine pattern of relative magnetic aromaticity alongside the non-nuclear magnetic shielding, i.e., the NICS.

COMPUTATIONAL METHODS

All structures were optimized by the Becke's three-parameter exchange[9] and Lee–Yang–Parr's correlation nonlocal functional[10] usually denoted B3LYP, combined with the 6-311++G(d,p) basis set.[11] Studying the second derivatives of energy confirmed that all geometries are true local minima on their corresponding potential energy hypersurfaces. Standard WFN protocols were prepared at the same computational level for subsequent topological analysis of the one-electron density,[12] studying the electron density and corresponding Laplacian. The saddle points of the electron density inside the molecular rings, i.e., ring critical points (RCPs) denoted as (3, +1) critical points, were found by the topological analysis of the electron density. The electron density, ρ, and its Laplacian, $\nabla^2\rho$, were computed at the RCP of each species as well as in 0.1 Å intervals above that point along an axis perpendicular to the molecular plane up to 5 Å above the ring plane. The $NICS_{zz}$ values were also computed at and above the RCP[13] in 0.1 Å intervals in the same points that the ρ and $\nabla^2\rho$ were computed. The RCP was chosen for the NICS calculations since this point has the lowest electron density in the ring plane, and previous studies confirm that employing the RCP instead of the nonweighted geometric center of the rings improves the consistency between the NICS values and other magnetic descriptors of aromaticity.[6e]

Although the NICS, ρ, and $\nabla^2\rho$ were scanned up to 5 Å above the ring planes of all species, the plots of ρ versus $NICS_{zz}$ and $\nabla^2\rho$ versus $NICS_{zz}$ in the subsequent section depict the values up to the height in which ρ and $\nabla^2\rho$ values are more than 0.0001 au in order to avoid, albeit conservatively, any random round-off errors in the ρ and $\nabla^2\rho$ calculations.

All topological analysis was done by the AIM2000[14] software, and the DFT calculations were performed by the Gaussian 98[15] suite of programs.

RESULTS AND DISCUSSION

The RCP and points close to it, e.g., the nonweighted geometric center, at the equilibrium geometries usually fall in the electron depletion zone of the molecular valence shell.[12] Accordingly, the computed $\nabla^2\rho$ values are positive at all considered RCPs as well as all the points above the RCP of a molecule perpendicular to its ring plane; this is true for both planar hydrocarbons as well as metallic/semimetallic species selected for this study. However, the observed patterns for the each class of species are discussed separately.

Hydrocarbons. Our recent investigations demonstrate that the magnetic aromaticity of aromatic hydrocarbons conform to a regular pattern; the strength of diatropic currents increases by increasing the number of π-electrons and, in the case of a fixed number of π-electrons, elevates by the increase in the ring size. This pattern emerges from two independent methodologies.[5f,6e] Having the same trend from two seemingly independent methodologies establishes a sound basis for the evaluation of the magnetic aromaticity order, especially when the results of these two approaches are in line with other standard methods.[5d,16]

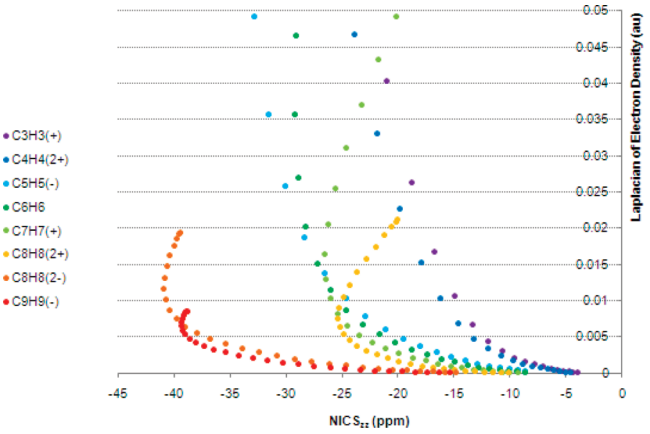

Figure 1. The plot of $\nabla^2\rho$ versus $NICS_{zz}$ for the eight considered hydrocarbons; in this plot, three groups of hydrocarbons with 2π-, 6π-, and 10π-electrons are distinguishable. As the number of electrons and the ring size are increased, the magnetic aromaticity also increases. Thus, more aromatic species shift toward the left-hand-side of this diagram.

Figure 1 depicts the plot of $\nabla^2\rho$ versus $NICS_{zz}$ for eight aromatic hydrocarbons. This Figure may be compared with Figure S-1 (Supporting Information), which depicts the plot of ρ versus $NICS_{zz}$ at the same computational level for the same set of molecules.[5f]

These two figures are apparently similar; three classes of aromatic molecules with 2π-, 6π-, and 10π-electrons are easily distinguishable in both figures. The overall pattern of the curves in Figure 1 is quite similar to that of Figure S-1, and the curvatures of all curves are toward the right; each curve consists of two ascending and descending parts in the high and low $\nabla^2\rho$ regions, respectively. As discussed previously,[5f] the lower parts of the curves (descending parts) are used for comparing the strength of diatropic π-currents in each molecule: the more the lower parts of the curves shift toward the left-hand side of the plot, the more aromatic the molecules. According to both Figures 1 and S-1, a cyclononatetraenyl anion with 10π-electrons and the largest ring size sustains the strongest diatropic currents. This is also in line with current intensity data obtained from our previous studies[6e] and the recently computed magnetizabilities by Pelloni and Lazzeretti.[16b] The relative magnetic aromaticity order of the 6π-electron species, cyclopentadienyl anion, benzene, tropylium cation, and cyclooctatetraene dication, is the same as that reported previously:[5c,6e,16] as the number of carbon atoms of the rings increases, the magnetic aromaticity increases slightly. Finally, the situation for the 2π-electron species in both figures is quite similar.

Thus, one may not find any considerable difference between the plots of $\nabla^2\rho$ versus $NICS_{zz}$ in contrast to that of the ρ versus $NICS_{zz}$, and it seems that both probes are of the same value for the considered hydrocarbons.

Bare Metallic and Semimetallic Clusters. Since the discovery of Al_4^{2-} in 2001[17] by Li et al. and the pioneering work of Fowler and his co-workers on analyzing the current density of this metallic cluster,[18] the term "all-metal aromatic" entered into chemical terminology. Although there are some accounts reporting the current density analysis of bare metallic clusters, the number of studied species is not diverse.[5d,18,19] Unfortunately, in

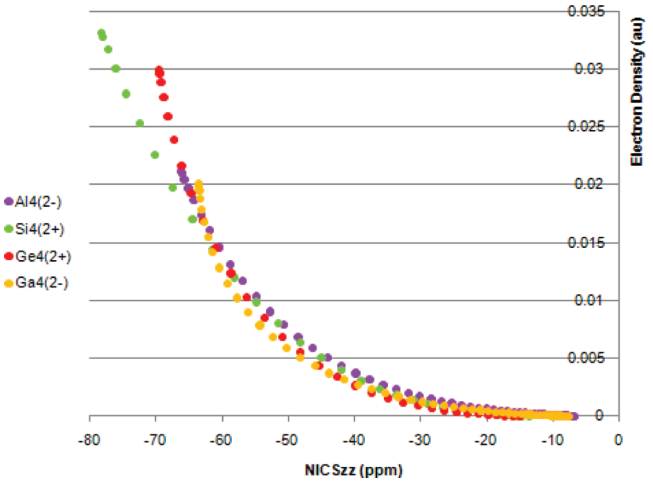

Figure 2. The plot of electron density, ρ, versus $NICS_{zz}$ for Al_4^{2-}, Si_4^{2+}, Ga_4^{2-}, and Ge_4^{2+}. Studying this plot suggests that the π-aromaticities of semimetallic clusters are more than those of metallic clusters; moreover, Al_4^{2-} is the least aromatic species among the studied species.

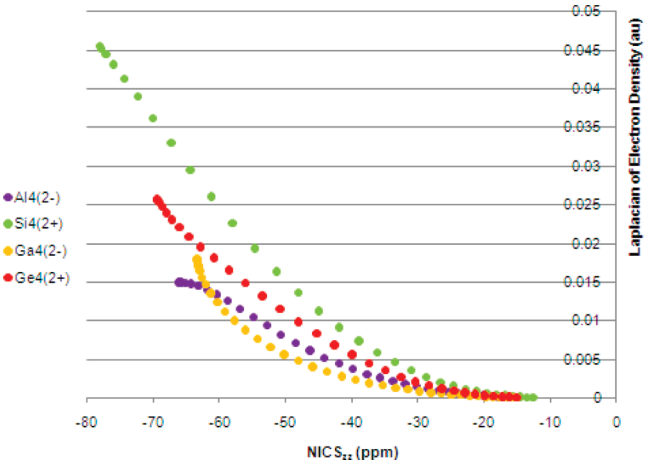

Figure 3. The plot of $\nabla^2\rho$ versus $NICS_{zz}$ scans for Al_4^{2-}, Si_4^{2+}, Ga_4^{2-}, and Ge_4^{2+}; the magnetic aromaticity order in this plot is the expected trend in line with previous studies. According to this plot, metallic clusters are more σ- and π-aromatic as their curves are shifted more toward the left-hand side.

these studies the quantitative strength of magnetic currents was not usually discussed, and the qualitative results cannot be used for a firm evaluation of our results herein.

However, in a recent paper we have measured the ring current intensity of 22 metallic and semimetallic clusters (M_4, M = Al, Si,[20] Ga,[21] Ge[22]) employing a ring current model based on classical electrodynamics.[6e] Although the model is a rather simple one, the good agreement between the predicted NICS values evaluated based on the proposed classical ring current intensity and the independent results of the NICS calculations as well as the current intensities obtained from the current density analysis methodology[5d] guarantees the reliability of the proposed ring current model.[6e] In the present study, the ring current intensity values obtained from the aforementioned model are used for the evaluation of the magnetic aromaticity order in metallic/semimetallic clusters emerged from considering the patterns of $\nabla^2\rho$ versus $NICS_{zz}$ scans.

Previous studies have shown that electron density distribution changes dramatically by changing the atom type in M_4 clusters (Figure S-2).[8g] In more electronegative and positively charged Si- and Ge-containing clusters, valence electrons are tightly distributed around the nuclei, and the electron density falls below 0.0001 au in distances not very far from the ring plane of the considered species (~3 Å above the ring plane electron density falls below the aforementioned threshold). Whereas, in Al- and Ga-containing clusters, where clusters are negatively charged, valence electrons are loosely bound, and the electron density smoothly decreases with increasing the distance from the ring plane (the electron density falls below 0.0001 au only above ~4.5 Å, far from the ring plane). This situation is basically different from that of the considered hydrocarbons, where in all species the electron density changes uniformly while the constituent atoms are the same.

The plots of electron density versus $NICS_{zz}$ for metallic/semimetallic clusters has a different shape compared with those of hydrocarbons (Figures 2 and S-3); in these plots, the $NICS_{zz}$ values decrease monotonically from the center of the cluster by decreasing the electron density. This feature is related to the double aromatic character of these species; in contrast to aromatic hydrocarbons, among the metallic/semimetallic clusters, the σ-framework sustains diatropic currents, and the $NICS_{zz}$ values around the ring plane are considerably negative.

The plot of electron density versus $NICS_{zz}$ for four pure metallic and semimetallic species, Al_4^{2-}, Si_4^{2+}, Ga_4^{2-}, and Ge_4^{2+} is presented in Figure 2 (similar plots for the rest of species are presented in Figure S-3). Studying the plots of electron density versus $NICS_{zz}$ for the metallic/semimetallic clusters is *not* helpful to discriminate the correct order of aromaticity in these species (Figures 2 and S-3). Studying the ring current intensities suggests that the relative order of magnetic aromaticity among these clusters is as follows: $Ga_4^{2-} > Al_4^{2-} > Ge_4^{2+} > Si_4^{2+}$.[6e] However, based on Figure 2, the ring current intensities of Ge_4^{2+} and Si_4^{2+} seem to be more than that of Al_4^{2-}. Moreover, considering the curves in the low electron density limit suggests that π-currents of semimetallic clusters are partially stronger than those of metallic clusters. Thus, these trends are in sharp contrast to the ring current intensities obtained from the previous study.[6e]

Studying the ring current intensities demonstrates that a number of M_3N clusters (M = Al or Ga, N = Si or Ge) are more aromatic than Ge_4^{2+} or Si_4^{2+}, while the plots of electron density versus $NICS_{zz}$ (Figure S-3) cannot verify this trend either. It has been demonstrated before that differences in the amount of the electron density in the ring center of aromatic hydrocarbons affects the single-point NICS results.[5f] It seems that the considerable differences in the electron density distribution among metallic/semimetallic clusters reduces the efficiency of the electron density versus $NICS_{zz}$ plots as a probe of magnetic aromaticity; the same factor that limits the application of single-point NICS also diminishes the reliability of the electron density versus $NICS_{zz}$ plots.

On the other hand, the patterns that emerge from the plots of $\nabla^2\rho$ versus $NICS_{zz}$ scans are completely different; Figure 3 depicts the plot of $\nabla^2\rho$ versus $NICS_{zz}$ scans for Al_4^{2-}, Si_4^{2+}, Ga_4^{2-}, and Ge_4^{2+}.

The general features of this plot are similar to those of the plots of the electron density versus $NICS_{zz}$ scan; the high-Laplacian part of the plot may be used to compare the σ-aromaticity of species, whereas in the low-Laplacian region, π-aromaticity manifests itself dominantly. The relative positions of the curves

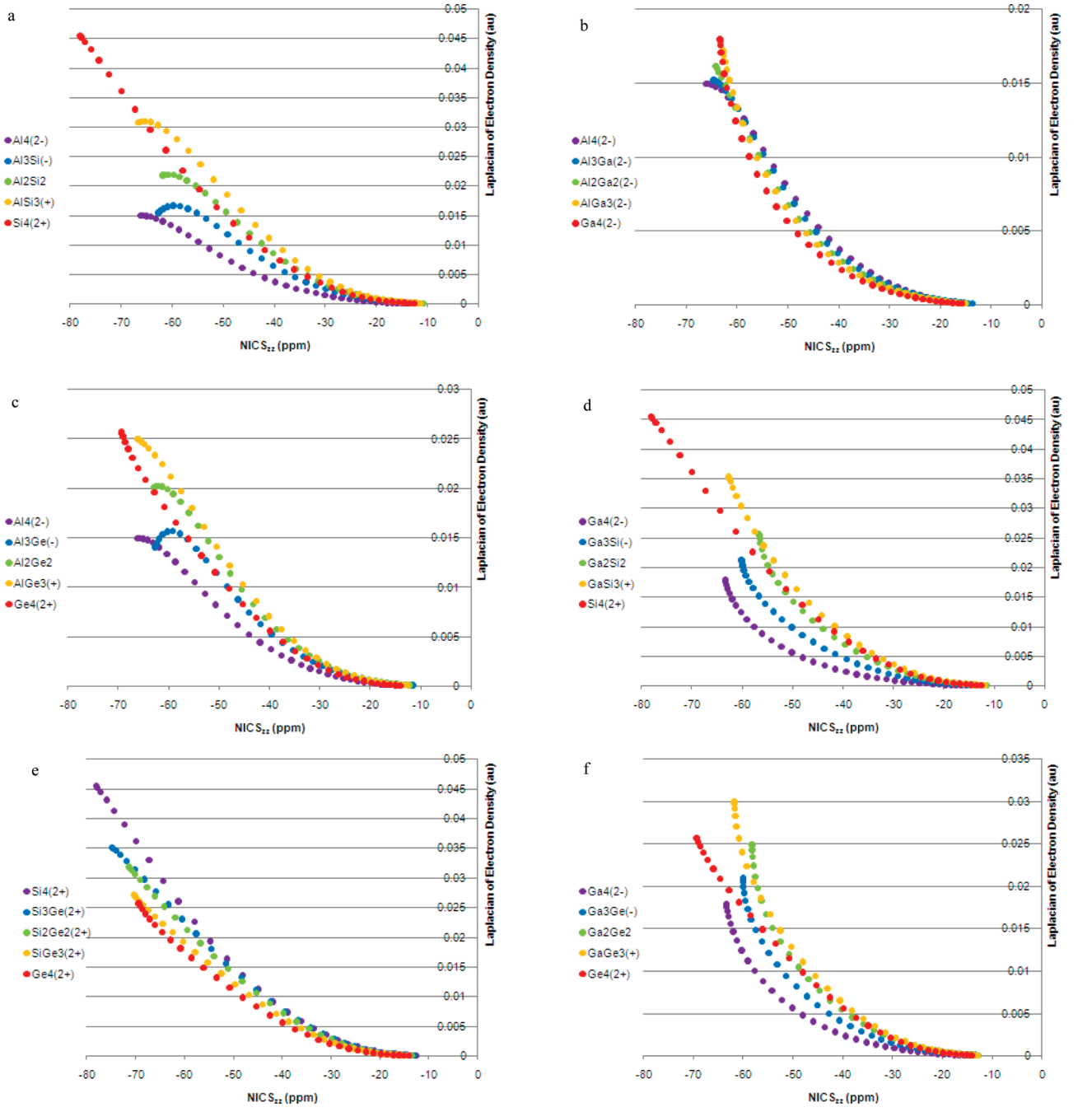

Figure 4. The plots of $\nabla^2\rho$ versus NICS$_{zz}$ scans for metallic/semimetallic clusters; pure metallic clusters are evidently more aromatic than other species in each group. In each plot, both the pure metallic and semimetallic clusters are presented in order to provide an unambiguous comparison with hybrid species.

in this plot are consistent with the expected trend from the current intensity studies. The curve of the most aromatic species, Ga_4^{2-}, is the first one on the left-hand side of this plot. The rest of the curves, from the left-hand side to the right-hand side, are associated with Al_4^{2-}, Ge_4^{2+}, and Si_4^{2+}; this order correlates well with the relative current intensity values, as the sums of the relative σ- and π-ring currents are 176, 168, 159, and 155 for Ga_4^{2-}, Al_4^{2-}, Ge_4^{2+}, and Si_4^{2+}, respectively.[6e]

Replacing atoms in each of the above-mentioned clusters with a heteroatom affects the relative current intensities. Generally, the substitution of heteroatoms reduces the relative current intensities, but according to current intensities[6e] in certain cases, hybrid clusters of type M_3N (M = Al, Ga; N = Si, Ge) are more aromatic than Si_4^{2+} or Ge_4^{2+}. Figure 4 depicts the plots of $\nabla^2\rho$ versus NICS$_{zz}$ scans for the hybrid clusters containing Al, Si, Ga, and Ge atoms. The relative position of the curves in the plots of Figure 4 is generally consistent with the relative current intensity values obtained from previous studies (see Table S-1). On the basis of these plots, pure metallic clusters are more aromatic than metallic−semimetallic hybrid clusters. By decreasing the number of metal atoms in each cluster, aromaticity decreases; pure semimetallic clusters are more aromatic than the hybrid clusters.

dx.doi.org/10.1021/jp203681x |*J. Phys. Chem. A* 2011, 115, 12708–12714

There are also exceptions among hybrid clusters: Ga_3Ge^- and Ga_3Si^- seem to be more aromatic than their corresponding pure semimetallic clusters.

Nevertheless, few differences are found in the relative position of curves in the high- and low-Laplacian regions of the plots and the relative current intensities; namely, relative σ- or π-aromaticity of some species are different according to ring current intensities, and the plots of $\nabla^2\rho$ versus $NICS_{zz}$ scans. According to current intensity values, both the σ- and π-current intensities of Al_3Si^- are less than that of Si_4^{2+}; Figure 4a shows that in the high-Laplacian region, i.e., σ-electrons, the curve of Al_3Si^- is placed on the left-hand side of the curve of Si_4^{2+}, suggesting that Al_3Si^- has a stronger σ-current than that of Si_4^{2+}. Studying the current intensity values shows that the σ-current intensities of Al_3Si^- and Si_4^{2+} are very similar. The same difference is found for Al_3Ga^{2-} and Al_4^{2-} as well as for Al_2Ge_2 and $AlGe_3^+$; in these cases, the differences in the current intensities are also negligible. On the other hand, in Figure 4e the curves of Si_3Ge^{2+} and $Si_2Ge_2^{2+}$ are placed on the left-hand side of the curve of Si_4^{2+} both in the high- and low-Laplacian zones (both σ- and π-currents); in these cases, the current intensities of clusters are also too low (the difference between the current intensities of $Si_2Ge_2^{2+}$ and Si_4^{2+} is quite small). Studying the position of the curves in the high-Laplacian region and low-Laplacian zone of the plots reveals a reasonable consistency with the current intensity values, as presented in Table S-1.

A precise study of the relative current intensities shows that discrepancies appear between the ring current intensities and the plots of $\nabla^2\rho$ versus $NICS_{zz}$ scans in cases where the difference between the ring current intensities of the two considered species is negligible. This small difference makes unambiguous order assignment questionable since the current intensities were defined based on a simplified ring current model; thus one hesitates to state conclusively which probe is more successful in determining the relative magnetic aromaticity unless these results are compared with the results of precise quantum current density analysis.

Evidently, the plots of $\nabla^2\rho$ versus $NICS_{zz}$ scans are useful for discriminating the aromaticity order among all-metal aromatic species. This approach has several advantages over the single-point NICS methodologies and the classical model of current intensity. As has been demonstrated before,[5f] single-point NICS methods cannot discriminate the aromaticity order of these species as they show that smaller rings, i.e., semimetallic clusters, are more aromatic than larger rings, i.e., metallic clusters. On the other hand, determining current intensity based on our ring current model, as introduced recently,[6e] seems to be a precise methodology that is in line with quantum current density analysis; however, this method requires time-consuming canonical molecular orbital NICS (CMO-NICS) analysis for a handful of points. The $\nabla^2\rho$ versus $NICS_{zz}$ scan is computationally much faster since it avoids the time-consuming CMO-NICS analysis. As it has been stated in the case of the electron density versus $NICS_{zz}$ scan,[5f] the $\nabla^2\rho$ versus $NICS_{zz}$ scan is not limited to single-determinant-based approaches, e.g., Hartree−Fock (HF) or DFT wave functions, and post-HF methods may also be used to compute both $\nabla^2\rho$ and $NICS_{zz}$ values as well, whereas orbital-based CMO-NICS methodology is useless in this domain.

The efficacy of $\nabla^2\rho$ versus $NICS_{zz}$ scan methodology may be better appreciated by another comparative example. Cyclononatetraenyl anion is the most aromatic species among the studied hydrocarbons; its relative π-current intensity (120.86) is comparable

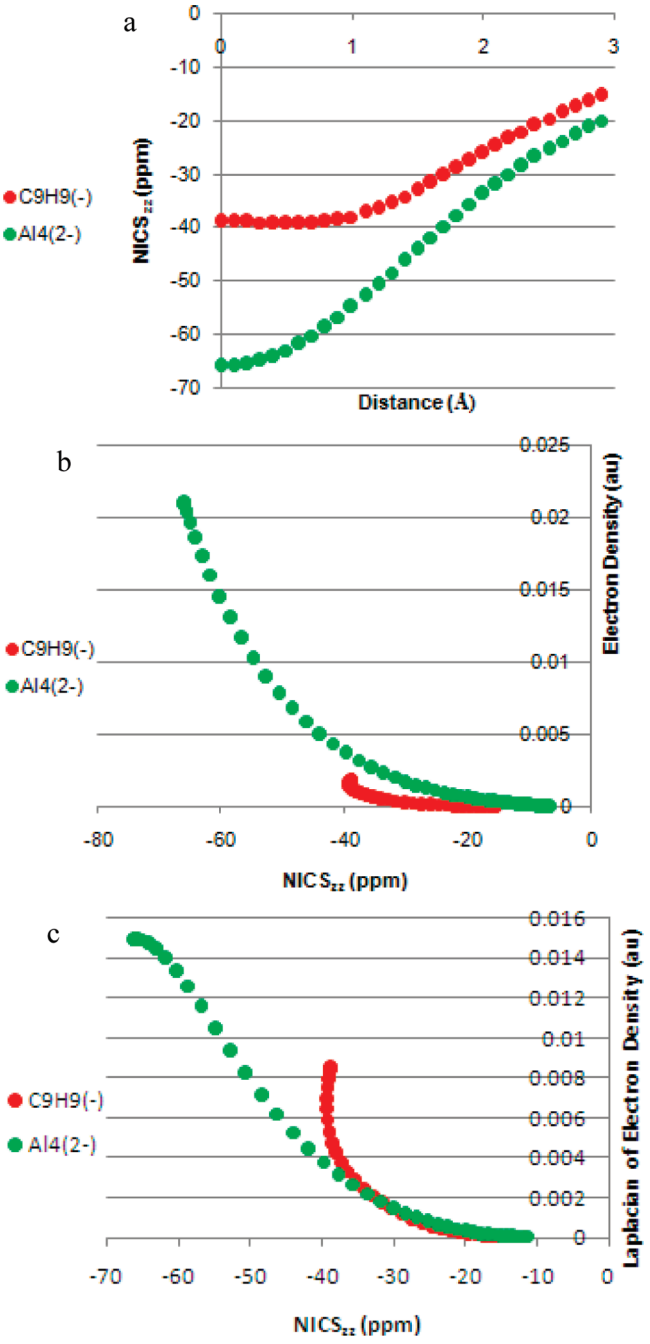

Figure 5. (a) $NICS_{zz}$ scan versus distance, (b) the plot of electron density versus $NICS_{zz}$ scan, and (c) the plot of $\nabla^2\rho$ versus $NICS_{zz}$ scan for cyclononatetraenyl anion and Al_4^{2-}. Relative current intensities of these species are not successfully verified by plots a and b, while plot c represents a realistic description.

with the σ-current intensity of Al_4^{2-} (141.77); π-aromaticity of Al_4^{2-} is not very considerable, as its relative π-current intensity is 26.30, and one may expect that in a reasonable distance above/below the ring planes of these two molecules, the diatropic π-currents of the cyclononatetraenyl anion are stronger than the sum of the π- and σ-currents of Al_4^{2-} (in Al_4^{2-}, σ-currents influence the non-nuclear shielding values up to distances far away from the ring plane[5d,19c]). A successful pictorial representation of aromaticity must verify the stronger π-currents of the

cyclononatetraenyl anion at large distances compared with the aluminum cluster, while demonstrating that the σ-aromaticity of Al_4^{2-} is also a strong factor in the magnitude of non-nuclear shielding values. Accordingly, conventional NICS scan methodology cannot verify the relative current intensities of Al_4^{2-} and the hydrocarbon since the $NICS_{zz}$ values of $C_9H_9^-$ remain less negative (smaller in absolute values) at all distances compared to those of Al_4^{2-} (Figure 5a).

On the other hand, the electron density distributions of aluminum cluster and the hydrocarbon are fundamentally different. In contrast to conventional NICS scans, studying the electron density versus $NICS_{zz}$ scan plot suggests that the cyclononatetraenyl anion is always considerably more aromatic than Al_4^{2-} (Figure 5b); this result is also not reliable. The correct trend is found in the plot of $\nabla^2\rho$ versus $NICS_{zz}$ scans for these species (Figure 5c); this plot shows that Al_4^{2-} is a strong σ-aromatic species, but the aromaticity of the hydrocarbon is comparable to that of Al_4^{2-} in the low-Laplacian region, i.e., the effect of π-currents of this hydrocarbon is more prominent than that of Al_4^{2-}, far from the ring plane of these molecules.

CONCLUSION

Although the exact relationship between one electron density and magnetic shielding is not straightforwardly established, it is generally appreciated that the differences in the electron density distribution among unlike molecules is one of the main sources of difference in the nuclear as well as non-nuclear magnetic shieldings. This effect particularly contaminates the NICS values when the constituent atoms of the systems under study are of different types, i.e., different nuclear charges, electronegativities, and atomic radii. The recently introduced electron density versus $NICS_{zz}$ scan approach could improve the conventional NICS scan methodology among similar molecules with different ring sizes; however, the issue for molecules with remarkable differences in electron density distribution remained unsolved (doubly charged anions must be considered cautiously as they are prone to auto electron detachment).[23]

The plot of $\nabla^2\rho$ versus $NICS_{zz}$ scans is a quick and reliable pictorial probe for studying the relative magnetic aromaticity among both hydrocarbons and metallic/semimetallic clusters; studying the behavior of the NICS aside from the Laplacian of the electron density instead of the electron density itself improves the efficiency of this methodology. This novel approach not only works well in the case of hydrocarbons but also performs reasonably successfully among all-metal aromatic clusters. Thus, one may claim that the efficiency of this approach is an intermediate between the simple single-point NICS or the orthodox NICS scan methodology and the sophisticated quantum current density analysis. Taking the fact that its computational cost and complexity is less than the quantum current density analysis, we advocate its use in computational studies that aim to probe the relative magnetic aromaticity among dissimilar series of species.

ASSOCIATED CONTENT

Supporting Information. Plot of electron density versus out-of-plane shielding for eight aromatic hydrocarbons; plot of electron density versus distance for Al_4^{2-}, Ga_4^{2-}, Si_4^{2+}, and Ge_4^{2+}; plots of electron density versus $NICS_{zz}$ for metallic/semimetallic clusters; and a table comparing the I_π, I_σ, I_{total}, $NICS(0)^{rcp}_{\sigma zz}$ and $NICS(0)^{rcp}_{\pi zz}$ values with $\nabla^2\rho$ versus $NICS_{zz}$ scan plots. This material is available free of charge via the Internet at http://pubs.acs.org.

AUTHOR INFORMATION

Corresponding Author

*E-mail: ranjbar@khayam.ut.ac.ir. Fax: 0098 21 6649 5291. Tel: +98 21 6111 3301.

REFERENCES

(1) (a) Kekule, A. *Bull. Acad. R. Belg.* **1860**, *10*, 347. (b) Breslow, R. *Acc. Chem. Res.* **1973**, *6*, 393.(c) Minkin, V. I.; Glukhovtsev, M. N.; Simkin, B. Y. *Aromaticity and Antiaromaticity. Electronic and Structural Aspects*; Wiley and Sons: New York, 1994. (d) *Chem. Rev.* **2001**, *101*, (5), 1115−1566. Special issue on aromaticity (Schleyer, P. v. R, Guest Ed). (e) *Chem. Rev.* **2005**, (10), *105*, 3433−3947. Special Issue on Delocalization—Pi and Sigma (Schleyer, P. v. R., Guest Ed). (f) Stanger, A. *Chem. Commun.* **2009**, 1939.

(2) (a) Boldyrev, A. I.; Wang, L.-S. *Chem. Rev.* **2005**, *106*, 3716. (b) Zubarev, D. Y.; Averkiev, B. B.; Zhai, H.-J.; Wang, L.-S.; Boldyrev, A. I. *Phys. Chem. Chem. Phys.* **2008**, *10*, 257.

(3) (a) Aihara, J.-I. *J. Phys. Org. Chem.* **2008**, *21*, 79. (b) Noorizadeh, S.; Dardab, M. *Chem. Phys. Lett.* **2010**, *493*, 376. (c) Giambiagi, M.; de Giambiagi, M. S.; dos Santos, C. D.; de Figueiredo, A. P. *Phys. Chem. Chem. Phys.* **2000**, *2*, 3381. (d) Bultinck, P.; Ponec, R.; Van Damme, S. *J. Phys. Org. Chem.* **2005**, *18*, 706. (e) Bultinck, P.; Rafat, M.; Ponec, R.; van Gheluwe, B.; Carbó-Dorca, R.; Popelier, P. *J. Phys. Chem. A* **2006**, *110*, 7642. (f) Fernández, I.; Frenking, G. *Faraday Discuss.* **2007**, *135*, 403. (g) Mandado, M.; Gonzalez, M. J.; Mosquera, R. A. *J. Comput. Chem.* **2006**, *28*, 127. (h) Matito, E.; Duran, M.; Solà, M. *J. Chem. Phys.* **2005**, *122*, 014109.Erratum: *J. Chem. Phys.* **2006**, *125*, 059901. (i) Perez-Juste, I.; Mandado, M.; Carballeira, L. *Chem. Phys. Lett.* **2010**, *491*, 224. (j) Koleva, G.; Galabov, B.; Wu, J. I-C.; Schaefer, H. F.; Schleyer, P. v. R. *J. Am. Chem. Soc.* **2009**, *131*, 14722. (k) Poater, J.; Fradera, X.; Duran, M.; Solà, M. *Chem.—Eur. J.* **2003**, *9*, 1113.

(4) (a) Chen, Z.; Wannere, C. S.; Corminboeuf, C.; Puchta, R.; Schleyer, P. v. R. *Chem. Rev.* **2005**, *105*, 3842. (b) Steiner, E.; Fowler, P. W.; Soncini, A.; Jenneskens, L. W. *Faraday Discuss.* **2007**, *135*, 309. (c) Matito, E.; Solà, M.; Salvador, P.; Duran, M. *Faraday Discuss.* **2007**, *135*, 325. (d) Merino, G.; Vela, A.; Heine, T. *Chem. Rev.* **2005**, *105*, 3812.

(5) (a) Xu, Q.; Jiang, L.; Tsumori, N. *Angew. Chem., Int. Ed.* **2005**, *44*, 4338. (b) Foroutan-Nejad, C.; Shahbazian, S.; Rashidi-Ranjbar, P. *Phys. Chem. Chem. Phys.* **2011**, *13*, 4576. (c) Fowler, P. W.; Soncini, A. *Chem. Phys. Lett.* **2004**, *383*, 507. (d) Monaco, G.; Zanasi, R.; Pelloni, S.; Lazzeretti, P. *J. Chem. Theory. Comput.* **2010**, *6*, 3343. (e) Stanger, A. *J. Org. Chem.* **2010**, *75*, 228. (f) Foroutan-Nejad, C.; Shahbazian, S.; Rashidi-Ranjbar, P. *Phys. Chem. Chem. Phys.* **2010**, *12*, 12630.

(6) (a) Schleyer, P. v. R.; Jiao, H.; Hommes, N. J. R. v. E.; Malkin, V. G.; Malkina, O. *J. Am. Chem. Soc.* **1997**, *119*, 12669. (b) Fowler, P. W.; Steiner, E. *Mol. Phys.* **2000**, *98*, 945. (c) Steiner, E.; Fowler, P. W.; Jennesskens, L. W. *Angew. Chem., Int. Ed.* **2001**, *40*, 362. (d) Lazzeretti, P. *Phys. Chem. Chem. Phys.* **2004**, *6*, 217. (e) Foroutan-Nejad, C.; Shahbazian, S.; Feixas, F.; Rashidi-Ranjbar, P.; Solà, M. *J. Comput. Chem.* **2011**, *32*, 2422.

(7) Schleyer, P. v. R.; Maerker, C.; Dransfeld, A.; Jiao, H.; Hommes, N. J. R. v. E. *J. Am. Chem. Soc.* **1996**, *118*, 6317.

(8) (a) Schleyer, P. v. R.; Manoharan, M.; Wang, Z. X.; Kiran, B.; Jiao, H.; Puchta, R.; Hommes, N. J. R. v. E. *Org. Lett.* **2001**, *3*, 2465. (b) Corminboeuf, C.; Heine, T.; Weber, J. *Phys. Chem. Chem. Phys.* **2003**, *5*, 246. (c) Heine, T.; Schleyer, P. v. R.; Corminboeuf, C.; Seifert, G.; Reviakine, R.; Weber, J. *J. Phys. Chem. A* **2003**, *107*, 6470. (d) Corminboeuf, C.; Heine, T.; Seifert, G.; Schleyer, P. v. R.; Weber, J. *Phys. Chem. Chem. Phys.* **2004**, *6*, 273. (e) Fallah-Bagher-Shaidaei, H.; Wannere, C. S.; Corminboeuf, C.; Puchta, R.; Schleyer, P. v. R. *Org. Lett.* **2006**, *8*, 863. (f) Stanger, A. *J. Org. Chem.* **2006**, *71*, 883. (g) Jiménez-Halla, J. O. C.; Matito, E.; Robles, J.; Solà *J. Organomet. Chem.* **2006**, *691*, 4359. (h) Stanger, A. *Chem.—Eur. J.* **2006**, *12*, 2745.

(9) (a) Becke, A. D. *J. Chem. Phys.* **1993**, *98*, 5648. (b) Becke, A. D. *Phys. Rev. A* **1988**, *38*, 3098.
(10) (a) Lee, C.; Yang, W.; Parr, R. G. *Phys. Rev. B* **1988**, *37*, 785. (b) Stephens, P. J.; Devlin, F. J.; Chabalowski, C. F.; Frisch, M. J. *J. Phys. Chem.* **1994**, *98*, 11623.
(11) (a) McLean, A. D.; Chandler, G. S. *J. Chem. Phys.* **1980**, *72*, 5639. (b) Krishnan, R.; Binkley, J. S.; Seeger, R.; Pople, J. A. *J. Chem. Phys.* **1980**, *72*, 650.
(12) Bader, R. F. W. In *Atoms in Molecules: A Quantum Theory*; Oxford University Press: Oxford, 1990.
(13) Morao, I.; Cossío, F. P. *J. Org. Chem.* **1999**, *64*, 1868.
(14) (a) Biegler-König, F. W.; Schönbohm, J.; Bayles, D. *J. Comput. Chem.* **2001**, *22*, 545. (b) Biegler-König, F. W.; Schönbohm, J. *J. Comput. Chem.* **2002**, *23*, 1489.
(15) Frisch, M. J.; Trucks, G. W.; Schlegel, H. B.; Scuseria, G. E.; Robb, M. A.; Cheeseman, J. R.; Zakrzewski, V. G.; Montgomery, Jr., J. A.; Stratmann, R. E.; Burant, J. C.; Dapprich, S.; Millam, J. M.; Daniels, A. D.; Kudin, K. N.; Strain, M. C.; Farkas, O.; Tomasi, J.; Barone, V.; Cossi, M.; Cammi, R.; Mennucci, B.; Pomelli, C.; Adamo, C.; Clifford, S.; Ochterski, J.; Petersson, G. A.; Ayala, P. Y.; Cui, Q.; Morokuma, K.; Malick, D. K.; Rabuck, A. D.; Raghavachari, K.; Foresman, J. B.; Cioslowski, J.; Ortiz, J. V.; Stefanov, B. B.; Liu, G.; Liashenko, A.; Piskorz, P.; Komaromi, I.; Gomperts, R.; Martin, R. L.; Fox, D. J.; Keith, T.; Al-Laham, M. A.; Peng, C. Y.; Nanayakkara, A.; Gonzalez, C.; Challacombe, M.; Gill, P. M. W.; Johnson, B.; Chen, W.; Wong, M. W.; Andres, J. L.; Gonzalez, C.; Head-Gordon, M.; Replogle, E. S.; Pople, J. A.; *Gaussian 98*; Gaussian, Inc.: Pittsburgh, PA, 1998.
(16) (a) Fowler, P. W.; Steiner, E. *J. Phys. Chem. A* **1997**, *101*, 1409. (b) Pelloni, S.; Lazzeretti, P. *J. Phys. Chem. A* **2011**, *115*, 4553. See the magnetizability data obtained from ab initio computations.
(17) Li, X.; Kuznetsov, A. E.; Zhang, H.-F.; Boldyrev, A. I.; Wang, L.-S. *Science* **2001**, *291*, 859.
(18) Fowler, P. W.; Havenith, R. W. A.; Steiner, E. *Chem. Phys. Lett.* **2001**, *342*, 85.
(19) (a) Havenith, R. W. A.; Fowler, P. W. *Chem. Phys. Lett.* **2007**, *449*, 347. (b) Lin, Y.-C.; Jusélius, J.; Sundholm, D. *J. Chem. Phys.* **2005**, *122*, 214308. (c) Havenith, R. W.; Fowler, P. W. *Phys. Chem. Chem. Phys.* **2006**, *8*, 3383.
(20) Zhai, H.-J.; Kuznetsov, A. E.; Boldyrev, A. I.; Wang, L.-S. *ChemPhysChem* **2004**, *5*, 1885.
(21) Kuznetsov, A. E.; Boldyrev, A. I.; Wang, L.-S. *J. Am. Chem. Soc.* **2001**, *123*, 8825.
(22) Nigam, S.; Majumder, C.; Kulshreshtha, S. K. *J. Mol. Struct. (THEOCHEM)* **2005**, *755*, 187.
(23) (a) Lambrecht, D. S.; Fleig, T. Sommerfeld. *J. Phys. Chem. A* **2008**, *112*, 2855. (b) Zubarev, D. Y.; Boldyrev, A. I. *J. Phys. Chem. A* **2008**, *112*, 7984. (c) Lambrecht, D. S.; Fleig, T.; Sommerfeld, T. *J. Phys. Chem. A* **2008**, *112*, 7986. (d) Dominikowska, J.; Palusiak, M. *J. Comput. Chem.* **2011**, *32*, 1441.